Aerodynamic challenge and limitation in long-span cable-supported bridges

* Yao-Jun Ge[1]

[1] *SLDRCE, Tongji University, Shanghai, 200092, China*
yaojunge@tongji.edu.cn

ABSTRACT

As one of the most formidable challenges on long-span cable-supported bridges, recent advances in wind engineering studies have been presented in the aspects of flutter instability, torsional divergence and stay cable vibration. Successful aerodynamic stabilization for long-span suspension bridges is reviewed, which is followed by current studies of several super long suspension bridges with a main span from 1680m in the 2nd Humen Bridge to 2016m in Sunda Strat Bridge. It seems that the intrinsic limit of span length due to aerodynamic stability is about 1,500m for a traditional suspension bridge, but slotted box deck could provide a 5,000m span length as the aerodynamic limit to a suspension bridge with high enough critical flutter and torsional speed. Since long-span cable-stayed bridge intrinsically has quite good aerodynamic stability based on close-box deck and spatial cables, rain-wind induced vibration and mitigation are discussed as a main aerodynamic challenge. In order to reveal the aerodynamic limit span length two super long cable-stayed bridges, with single 1400m span and double 1500m spans in Qiongzhou Strait Bridge, have been experimentally investigated through sectional and full models in flutter and torsional instability.

1. INTRODUCTION

Cable-supported bridge can be defined as a bridge with the deck supported by hangers or cables, which are held up by pylons or main cables, and accordingly divided into two kinds, suspension bridge with greater bridging capacity and cable-stayed bridge. The evolution and achievements of bridging capacity of these two kinds of cable-supported bridges greatly promote the development of modern bridge engineering and advanced bridge aerodynamics.

Although ancient suspension bridges were built in China long before the history of the Anno Domini, the construction of modern suspension bridges around the world has experienced a considerable development since 1883, when the first modern suspension bridge, Brooklyn Bridge, was built. It took about 48 years for the span

---

[1] Professor

length of suspension bridges to grow from 486m of Brooklyn Bridge to 1067m of George Washington Bridge in 1931, as the first bridge with a span length over 1,000m, and had a great increase factor of 2.2. Although the further increase in the next 50 years to Golden Gate Bridge of 1280m, Verrazano Bridge of 1298m and Humber Bridge of 1410m in 1981 was only 1.3, another factor of about 1.4 was realized in Akashi Kaikyo Bridge with a 1,991m span greater than that of Great Belt Bridge within 17 years in 1998. Fig. 1 shows the suspension bridges with a record-breaking span length in the history after Brooklyn Bridge (Ge and Xiang 2008).
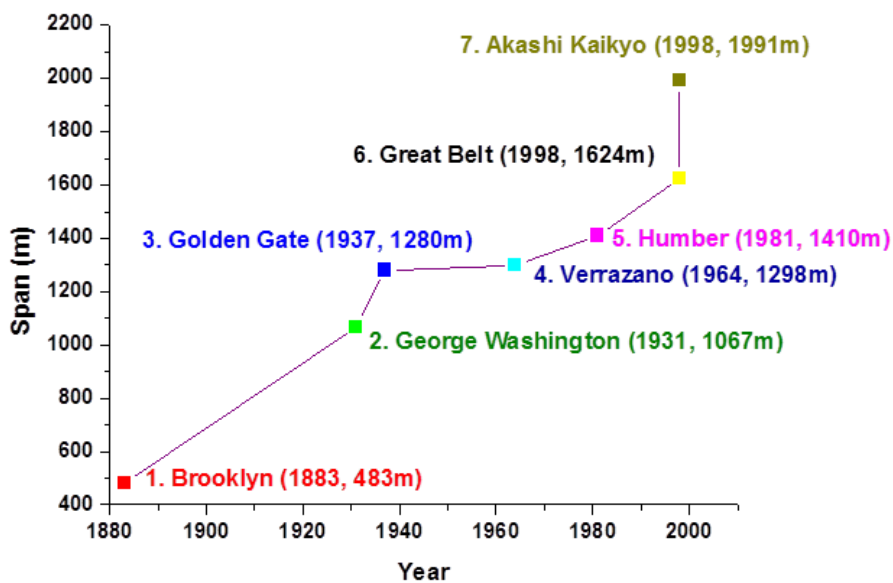

Fig. 1 Record-breaking suspension bridges

Cable-stayed bridges can be traced back to the 18th century, and many early suspension bridges were of hybrid suspension and cable-stayed construction, for example, Brooklyn Bridge. The steel-decked bridge, Stromsund Bridge completed in 1955, is often cited as the first modern cable-stayed bridge with a main span of 183m. It took about 20 years for the span length of cable-stayed bridges to enlarge to 404m in Saint-Nazaire Bridge in 1975 with an increase factor of 2.2, and the same increase factor was achieved within next 24 years in the 890m Tatara Bridge in 1989 after the 440m Barrioscle Luna Bridge, the 465m Annacis Bridge, the 520m Skamsund Bridge, the 602m Yangpu Bridge and the 856m Normandy Bridge. Another big jump with about two hundred meters in span length was realized in the 1088m Sutong Bridge in 2008 and the 1104m Russky Bridge in 2012. Fig. 2 gives the recording breaking cable-stayed bridges in the history (Ge and Xiang 2008).
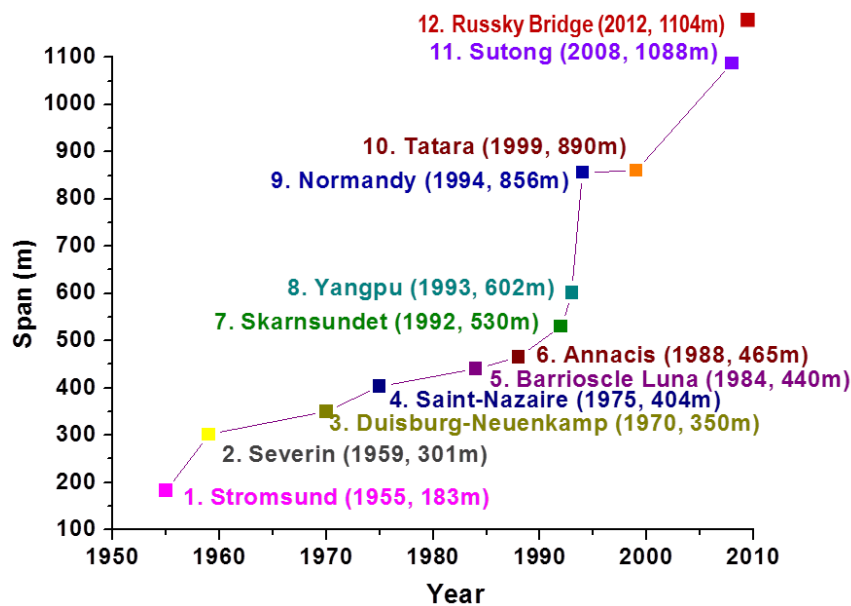
Fig. 2 Record-breaking cable-stayed bridges

As a human dream and an engineering challenge, the structural engineering of bridging larger obstacles has entered into a new era of crossing wide rivers and sea straits, including Tsugaru Strait in Japan, Qiongzhou Strait and Taiwan Strait in China, Sunda Strait in Indonesia, Messina Strait in Italy, Gibraltar Strait linking European and African Continents, and so on. One of the most challenging aspects has been identified as bridging capacity, for example, 1,500m span for Qiongzhou Strait, 2016m for Sunda Strait and 5,000m for Taiwan Strait. With super long span length, cable-supported bridges are becoming lighter, more flexible, and lower damping, which result in more sensitive to wind actions related to torsional divergence, flutter instability, frequent buffeting response, large amplitude vortex induced vibration (VIV), severe rain-wind induced vibration (RWIV) of stay cables, and so on. Among them, the most challenging aerodynamic concerns for cable-supported bridges with super long span are aerodynamic flutter instability, aerostatic torsional divergence and cable RWIV, which have been discussed in this paper.

2. SUCCESSFUL STABILIZATION IN LONG-SPAN SUSPENSION BRIDGES

Ten longest-span suspension bridges completed in the world are listed in Table 1, including five in China and one in Japan, Denmark, Korea, UK and Norway, respectively (Internet address A 2016). Among these ten suspension bridges, seven of them have encountered aerodynamic problems including five in flutter and two in VIV. Both Great Belt Bridge and the 4th Nanjing Bridge have simply used guide vanes to improve VIV, and the other five bridges suffered in flutter have adopted three kinds of control measures, including stabilizer, twin box or slot and their combination, which are discussed as successful stabilization in the following sections.

Table 1 Ten longest-span suspension bridges completed in the world

Span Order	Bridge Name	Main Span	Girder Type	Wind-Induced Problem	Control Measure	Country	Year Built
1	Akashi Kaikyo	1991m	Truss	Flutter	Slot/Stabilizer	Japan	1998
2	Xihoumen	1650m	Box	Flutter	Twin box	China	2009
3	Great Belt	1624m	Box	VIV	Guide vane	Denmark	1998
4	Yi Sun-sen	1545m	Box	Flutter	Twin box	Korea	2012
5	Runyang	1490m	Box	Flutter	Stabilizer	China	2005
6	4th Nanjing	1418m	Box	VIV	Guide vane	China	2012
7	Humber	1410m	Box	No	None	UK	1981
8	Jiangyin	1385m	Box	No	None	China	1999
9	Tsing Ma	1377m	B/T	Flutter	Slot	China	1997
10	Hardanger	1310m	Box	No	None	Norway	2013

2.1 Central stabilizer in Runyang Bridge

Among the top ten suspension bridges in Table 1, Runyang Bridge across Yangtze River in China completed in 2005 is the second longest suspension bridge in China and the fifth longest in the world. The main section of the bridge was designed as a typical three-span suspension bridge with the span arrangement of 510m + 1490m + 510m and the deck cross section of 36.3m width and 3m depth, as shown in Fig. 3.

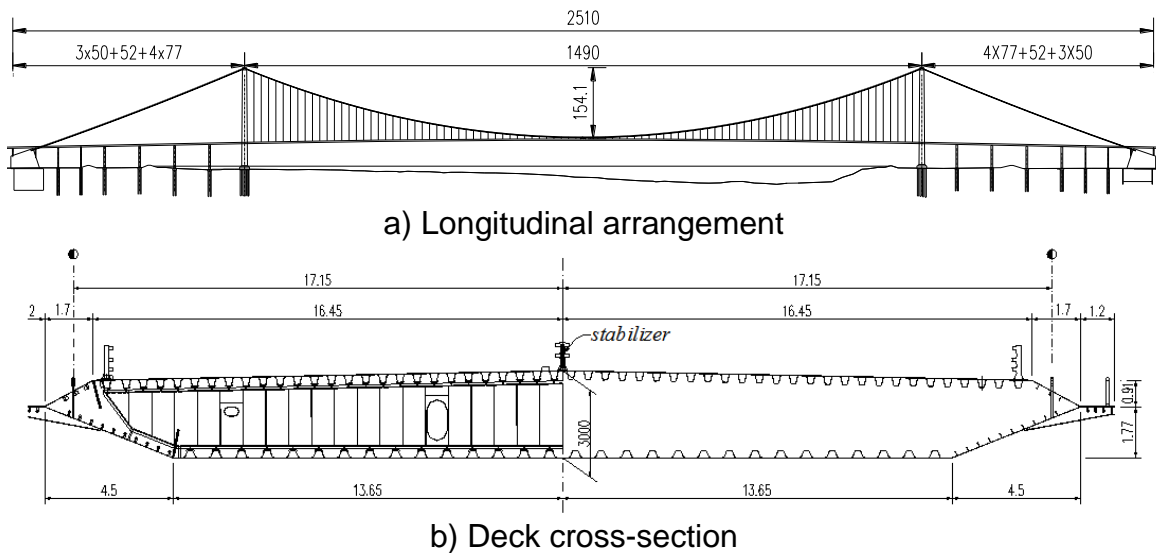a) Longitudinal arrangement

b) Deck cross-section

Fig. 3 Runyang Bridge across Yangtze River (Unit: m)

In order to investigate aerodynamic flutter, a wind tunnel experiment with a 1:70 sectional model was carried out in the TJ -1 Boundary Layer Wind Tunnel in Tongji University. It was found in the first phase of the testing that the original structure could not meet the requirement of checking flutter speed of 54m/s. Some preventive means had

to be considered to stabilize the original structure. With a stabilizer in the center of the bridge deck, further sectional model testing was conducted, and the confirmation wind tunnel tests with a full aeroelastic model were also performed in TJ-3 Boundary Layer Wind Tunnel with the working section of 15m width, 2m height, and 14m length. The critical flutter speeds obtained from the sectional model (SM) and the full model (FM) wind tunnel tests are collected and compared in Table 2. Both experimental results show good agreement with each other and the central stabilizer of 0.88 m height as shown in Fig. 4 can raise the critical flutter speed over the required value (Chen et al., 2002).

Table 2 Critical flutter speed of Runyang Bridge

Deck box girder	Critical flutter speed (m/s)				Required
Configuration	SM at 0°	FM at 0°	SM at +3°	FM at +3°	(m/s)
Original box girder	64.4	64.3	50.8	52.5	54
With a 0.65m stabilizer		69.5	58.1	53.8	54
With a 0.88m stabilizer		72.1	64.9	55.1	54
With a 1.1m stabilizer		>75	67.4	56.4	54

Fig. 4 Central stabilizer mounted on Runyang Bridge

2.2 Twin box girder in Xihoumen Bridge

Xihoumen Sea-Crossing Bridge is part of the Zhoushan Island-Mainland Connection Project linking Zhoushan Archipelago and Ningbo City in Zhejiang Province, China. The bridge route is selected at the shortest distance of the Xihoumen Strait between Jintang Island and Cezi Island, about 2200 m far away. Between these two islands and near Cezi, there is a small island, called Tiger Island, which can be used to hold on a pylon for a cable-supported bridge. In order to avoid from constructing deep-water foundation, Xihoumen Bridge is designed as a two-continuous-span suspension bridge with the span arrangement of 578m + 1650m + 485m shown in Fig. 5.
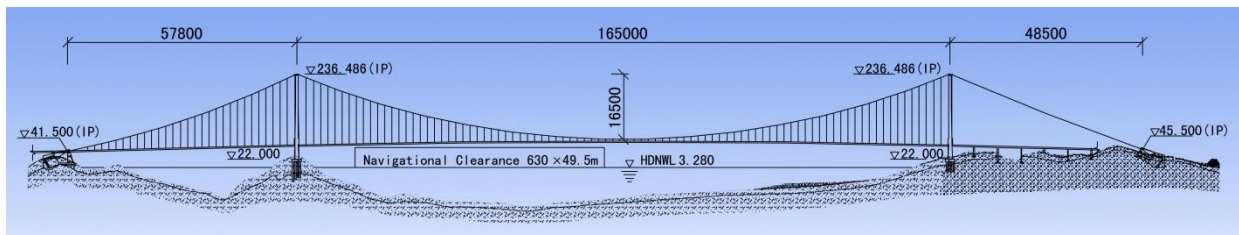
Fig. 5 Longitudinal arrangement of Xihoumen Bridge (Unit: cm)

Based on the experience gained from the 1490m Runyang Bridge with critical flutter speed of 51 m/s and the 1624 m Great Belt Bridge with 65 m/s critical speed, the span length of 1650 m may suffer with aerodynamic instability for suspension bridges, even with the stricter stability requirement of 78.4 m/s in Xihoumen Bridge located in typhoon prone area. Besides traditional single box girder (Fig. 6a) and the box girder with a central stabilizer (Fig. 6b), two more twin box girders with a central slot of 6m (Fig. 6c) and 10.6m (Fig. 6d), were investigated through sectional model wind tunnel testing.

(U_{cr} = 46.2m/s)
a) Traditional single box

(U_{cr} = 88.0m/s)
b) With a 2.2m central stabilizer

(U_{cr} = 88.4m/s)
c) Twin box with a 6m slot

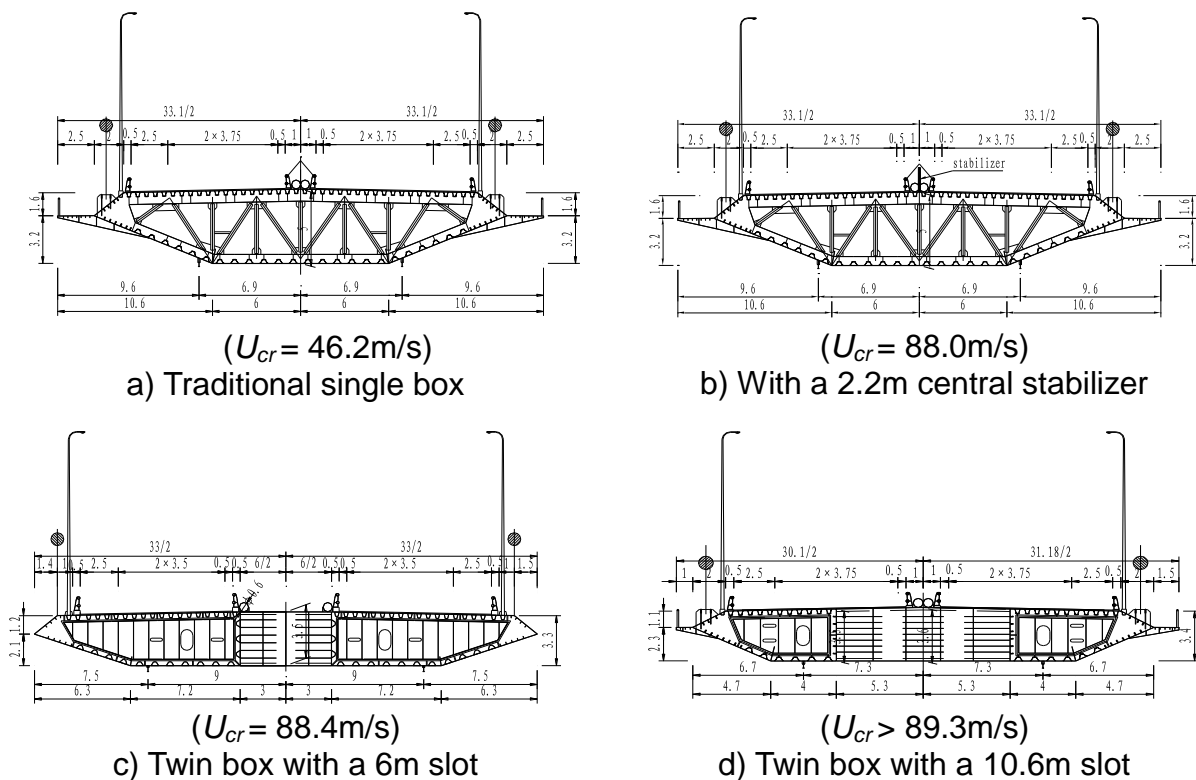(U_{cr} > 89.3m/s)
d) Twin box with a 10.6m slot

Fig. 6 Alternative box-girder sections for Xihoumen Bridge

The experimental results of critical flutter speeds are summarized for these four cross section girders in Table 3. Apart from the traditional single box, the rest three cross sections, including the box girder with a 2.2m central stabilizer, the twin box girders with a 6m and 10.6m slot, can meet with the flutter stability requirement under

the attack angles of -3°, 0° and +3°. The twin box girder with a 6m slot was finally selected as the proposed scheme, which was further modified to the final configuration as shown in Fig. 7 (Ge et al., 2003). Twin box girder has been firstly adopted for the purpose of aerodynamic stabilization in Xihoumen Bridge in China in 2009, and followed by Yi Sun-sen in Korea in 2012.

Table 3 Critical flutter speeds of Xihoumen Bridge

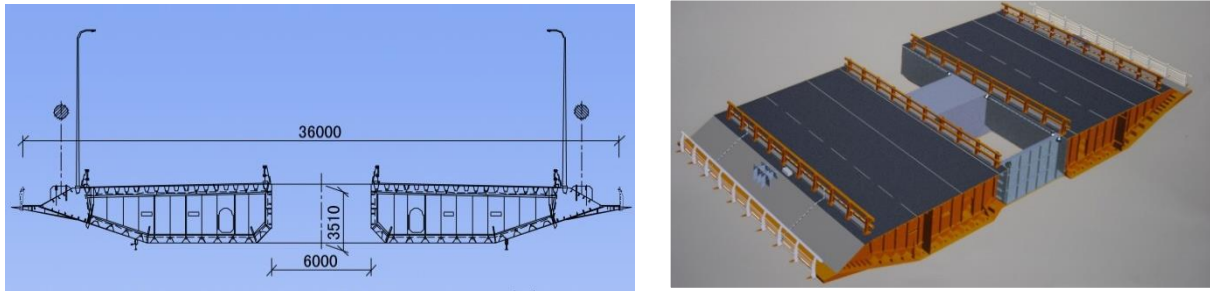| Deck box girder	Critical flutter speed (m/s)				Required
Configuration	−3°	0°	+3°	Minimum	(m/s)
Single box girder	50.7	46.2	48.7	46.2	78.4
Single box with 2.2m stabilizer	>89.3	>89.3	88.0	88.0	78.4
Twin boxes with 6m slot	88.4	>89.3	>89.3	88.4	78.4
Twin boxes with 10.6m slot	>89.3	>89.3	>89.3	>89.3	78.4

Fig. 7 Twin box girder of Xihoumen Bridge

2.3 Combination of stabilizer and slot in Akashi Kaikyo Bridge

The Akashi Kaikyo Bridge is one part of the Honshu-Shikoku Highway Project, crossing the busy Akashi Strait, and linking the city Kobe and the island Awaji. To ensure enough safety for the 1.5km wide international navigation channel below, the arrangement of the bridge span is set as 960m + 1991m + 960m, shown in Fig. 8. Its construction began in April 1988, and was opened for traffic exactly ten years later in April 1998. Since its completion, it has been the world's record of having the longest central span of any suspension bridges.
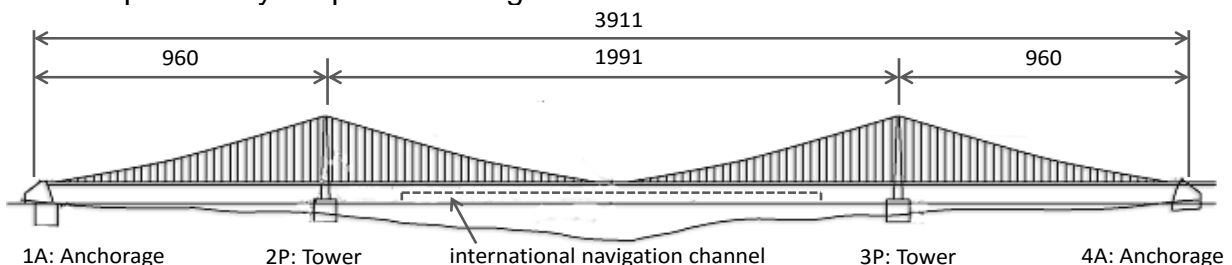

Fig. 8 Longitudinal arrangement of Akashi Kaikyo Bridge (Unit: m)

According to the Japanese code, the checking flutter speed is set to 78m/s considering the local wind environment. This makes it a severe problem to design an appropriate stiffening girder, whose aerodynamic stability must be good enough to satisfy the required checking wind speed, with such an extremely flexible structure. Substantial efforts had been made to optimize the aerodynamic shape of the girder. Several girder types were examined by sectional model and also numerical analysis, shown in Fig. 9 (Makoto, 2004).
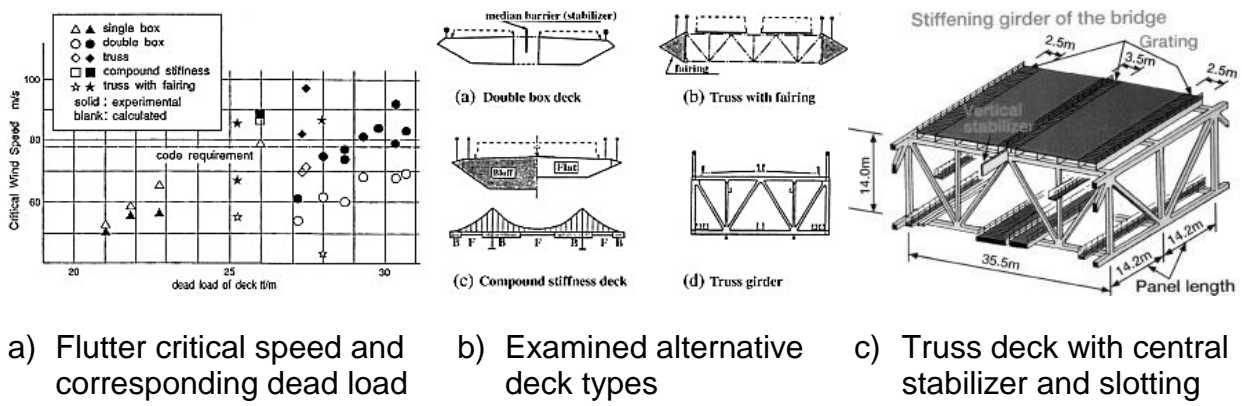
a) Flutter critical speed and corresponding dead load	b) Examined alternative deck types	c) Truss deck with central stabilizer and slotting

Fig. 9 Aerodynamic flutter optimization of the bridge's deck.

Truss girder with central stabilizer and slotting was finally selected, shown in Fig. 9c, due to both the wind-resistant requirement and the erection process. On one hand, a simple truss girder without any control measures cannot provide sufficient stability under the checking wind speed. Installation of a vertical stabilizer upon the upper road deck and slotting of the lower road deck were found to be necessary. On the other hand, it is convenient to introduce the cantilever erection method. The girder can be constructed starting from the tower without interrupting the sea traffic, rather than lifting the girder block from the navigation channel if steel box girder were used (Miyata, 2003).

As a final check of the overall flutter stability of the bridge structure, wind tunnel tests with a full aeroelastic model were carried out, shown in Fig. 10 (Miyata, 2003). The involved three-dimensional characters were thus considered, like the varying torsional deflection along the bridge axis, the spatial correlation of the wind field, and the interference between the cables and the girder, et al. It was found that the stabilizer could be restricted to the center span only, giving a much more economical solution. At that time, it also provided evidences of the accuracy of numerical calculation, helping the Finite-Element-Method (FEM) widely used in flutter analysis nowadays.
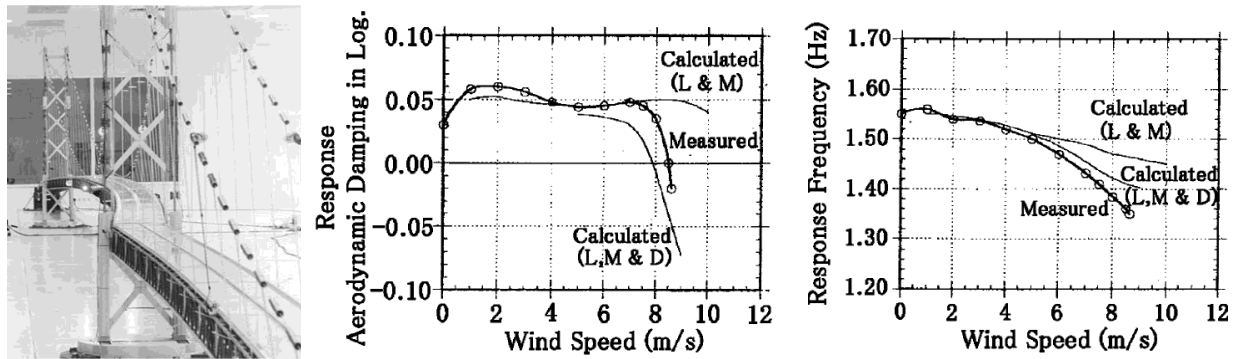
Fig. 10 Response of a 1/100 full aeroelastic model with wind tunnel speed.

3. CHALLENGING STABILIZATION FOR SUPER-LONG SUSPENSION BRIDGES

Eight super-long suspension bridges proposed in the world are listed in Table 4, with a steel box or truss stiffening girder span from 1658m to 5000m under feasibility study, working design or substructure construction. Among these eight suspension bridges, six of them have encountered aerodynamic flutter problems, and almost all design schemes have adopted slotted box girders with twin or triple boxes. Three typical super-long span suspension bridges, including Shuangyumen Bridge, Sunda Strait Bridge and Taiwan Strait Bridge, which have been studied in Tongji University, are discussed as challenging stabilization in the following sections.

Table 4 Super-long suspension bridges under construction or design or proposal

Span Order	Bridge Name	Main Span	Girder Type	Wind-Induced Problem	Control Measure	Country	Stage Built
1	Shenzhong	1658m	Box	Flutter	Twin-box	China	Design
2	2nd Humen	1688m	Box	No	None	China	Constr.
3	Yangsigang	1700m	Truss	No	None	China	Constr.
4	Shuangyumen	1708m	Box	Flutter	Twin-box	China	Feasibility
5	Sunda Strait	2016m	Box	Flutter	Twin-box	Indonesia	Feasibility
6	Messina Strait	3300m	Box	Flutter	Triple-box	Italy	Design
7	Gibraltar Strait	3500m	Box	Flutter	Twin-box	Spain/ Morocco	Feasibility
8	Taiwan Strait	5000m	Box	Flutter	Twin-box	China	Feasibility

3.1 Single or twin box girder in Shuangyumen Bridge
Located in the Zhoushan Archipelago in the East China Sea, Shuangyumen Bridge was preliminarily designed as a suspension bridge with a single span of 1708m, shown in Fig. 11. Due to the adverse wind environment at the bridge site, the flutter checking wind speed is over 80m/s, which makes aerodynamic instability the primary

concern for designers and researchers. Two possible girder schemes were proposed, single box girder with the central stabilizer (Section 1) and twin box girder (Section 2).
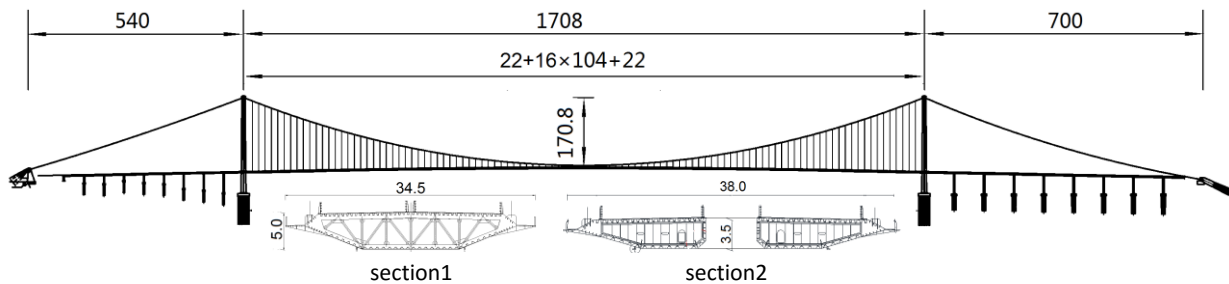

Fig. 11 General layout and alternative box deck sections

The purpose of the first scheme is trying to achieve a better VIV performance than twin box girders. Since the flutter critical speed of the original single box girder is only 69.2m/s without the help of vertical stabilizers, various central stabilizers, above or below the girder, with different plate heights and under different wind attack angles, were tested to explore the best flutter control effect.

An upper stabilizer above the girder is most common choice, such as in Runyang Bridge (Fig. 4). Both numerical simulation and wind tunnel tests indicate that the flutter critical speed first increase and then drop with the increase of upper stabilizer height, H_a, which implies the existence of an optimal stabilizer height. This tendency was confirmed in the further investigation by sectional model wind tunnel tests as shown in Table 5. The optimal stabilizer height, 14% of the girder depth, H, can be determined from the test results. It should be noted that there is a transition of the most unfavorable wind attack angle from -3° to 0° from $H_a/H = 0.14$ to $H_a/H = 0.17$ (Ge et al., 2015).

Table 5 Flutter critical speed of single box girder with single upper stabilizer

Control measure	H_a/H	+3°(m/s)	0°(m/s)	-3°(m/s)	Min(m/s)	Critical wind speed
Single upper stabilizer	0.00	76.7	84.5	69.2	69.2	
	0.10	84.0	83.9	81.2	81.2	
	0.14	**85.1**	**83.6**	**83.3**	**83.3**	
	0.17		82.4	83.3	82.4	
	0.20	87.4	80.2	84.5	80.2	
	0.24	86.0	79.3	83.3	79.3	
	0.28	86.0	77.7	83.3	77.7	
	0.32	86.8		87.7		
	0.36	86.2		85.1		
	0.40	84.8		85.1		
	0.44	84.5				
	0.50	84.2				
	0.60	83.0				

One disadvantage of upper vertical stabilizer may be the compromise of the field vision of motorists. In this sense, lower stabilizer below the girder can be a better solution. Their flutter control effects on single box girder from sectional model wind

tunnel tests are summarized in Table 6. The optimal stabilizer height is shifted to 17% of the girder depth.

Table 6 Critical flutter wind speed single box girder with single lower stabilizer

Control measure	Hb/H	+3°(m/s)	0°(m/s)	-3°(m/s)	Min(m/s)	Critical wind speed
Single lower stabilizer	0.00	76.7	84.5	69.2	69.2	
	0.10		86.9	73.0	73.0	
	0.14	80.5	87.1	92.7	80.5	
	0.17	**80.9**	**88.3**	**95.6**	80.9	
	0.20	77.0	87.4	94.3	77.0	
	0.24		84.2	89.3		
	0.32	69.1				

In order to further improve the aerodynamic stability performance, the combination of upper and lower stabilizer has been tried, and the results of flutter critical speeds are illustrated in Fig. 12. According to the testing results, the combination of upper stabilizer with the height of 24% girder depth and lower stabilizer with the height of 17% girder depth has the best flutter performance. In that case, the flutter critical wind speed is 89.1m/s, with a raise of 29% compared to the original section, 7% to the optimal single upper stabilizer and 10% to single lower stabilizer (Ge et al., 2015).
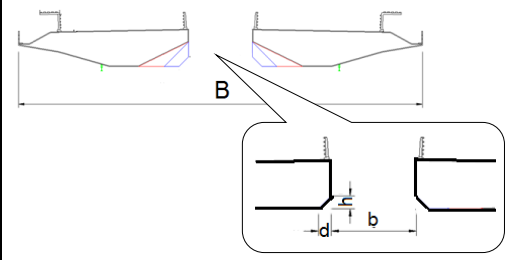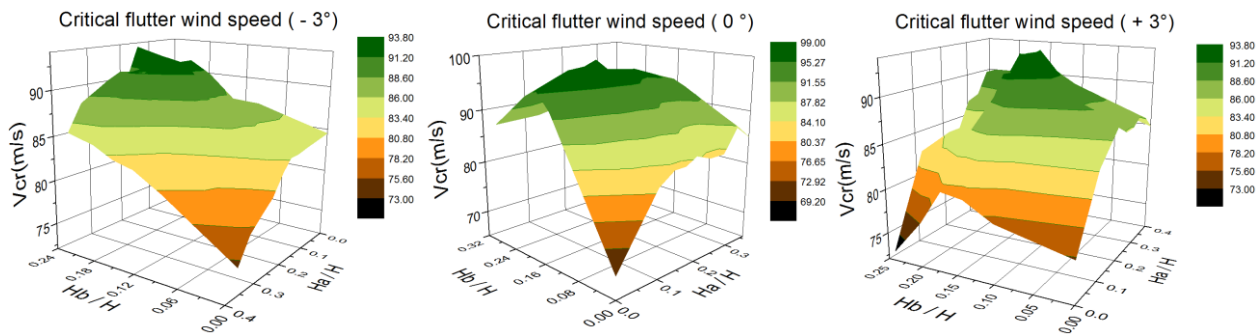

Fig. 12 Flutter critical wind speed with combined vertical stabilizers

As far as flutter performance is concerned, twin box girder is a better solution compared with single box girder. In this investigation, the slotting width ratio, *b*/*B*, and the chamfering size, *h*×*d*, of the inner corner were selected as shape optimization parameters, the results from sectional model wind tunnel tests are listed in Table 7.

Table 7 Flutter critical wind speed of twin box girder with different chamfering sizes

b/B(m/m)	h×d (m×m)	Flutter wind speed (m/s)			Minimum speed (m/s)	
		-3°	0°	+3°		
5 / 37	0.9×0.9	89.6	>100	>100	89.6	
5.5 / 37.5	0.9×0.9	91.8	>100	>100	91.8	
6 / 38	0.9×0.9	92.4	>100	>100	92.4	
6 / 38	2.3×2.3	94.1	>100	>100	94.1	
6 / 38	4.7×2.3	95.2	>100	>100	95.2	

As the results shown in Table 7, the flutter performance is improved by the increasing of slot width ratio as the chamfering size of inner corner is fixed to $h{\times}d$ = 0.9×0.9m, while the enlarging of inner corner chamfering will also increase the flutter critical wind speed. However, all five cases have a critical wind speed higher than 89.6m/s, which suggests that central slot has certain superiority in the flutter control domain.

3.2 Deep or shallow twin box girder in Sunda Strait Bridge

As a main part of the Trans Asian & Asean Highway and Railway in Indonesia, Sunda Strait Bridge linking Sumatra Island and Java Island is planned as a super-long span suspension bridge with the span arrangement of 792+2016+792m and the cable sag to span ratio of 1/10 as shown Fig. 13. In the conceptual design stage, there are two stiffening girder design schemes provided by the designers, that is, the deep twin box girder in Fig. 14 and the shallow twin box girder in Fig. 15. The deep twin box girder is 51.8m wide and 9.76m deep with a central slot width of 2.25m, and the shallow one is 60.35m wide and 5.8m deep with a slot of 10.8m. The ventilation ratios of these two girders can be calculated by dividing net slot area by total slot area, and have the values of 31% in the deep scheme and 53% in the shallow scheme, respectively, which are very important to aerodynamic flutter stability (Zhou et al., 2015a).
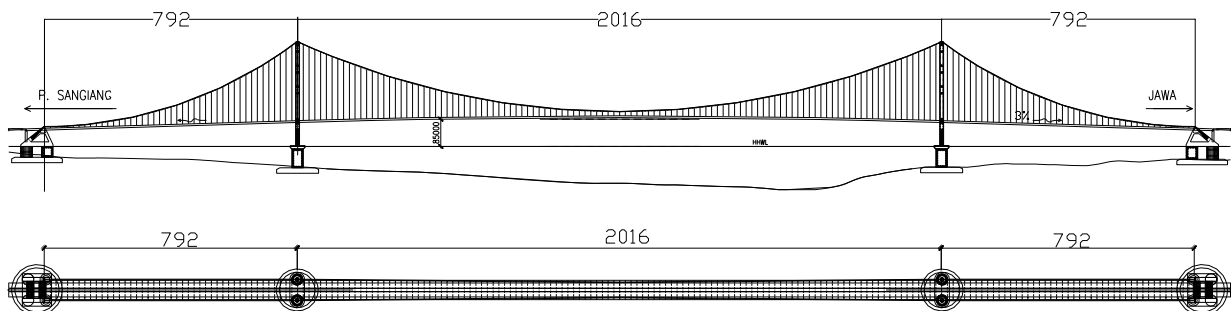

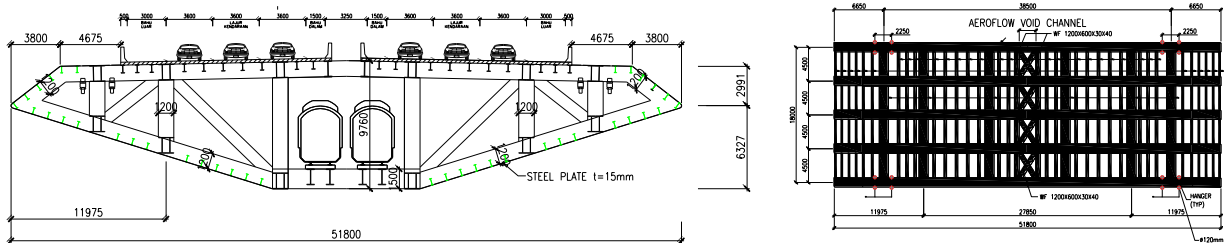Fig. 13 Longitudinal arrangement of Sunda Strait Bridge (Unit: m)

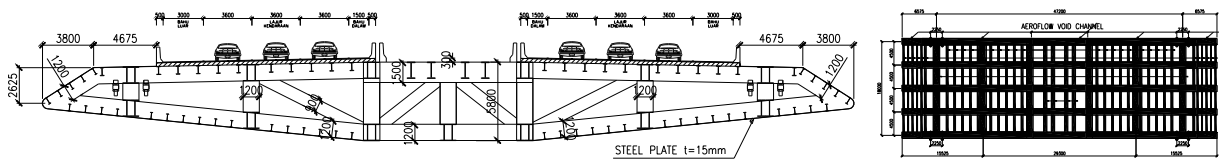Fig. 14 Deep twin box girder of Sunda Strait Bridge

Fig. 15 Shallow twin box girder of Sunda Strait Bridge

Having performed a structural dynamic finite-element analysis on Sunda Strait Bridge design schemes, the fundamental natural frequencies of both deep and shallow twin box girder schemes have been compared in Table 8, and the equivalent mass and mass moment have been listed in Table 9 (Zhou et al., 2015a).

Table 8 Fundamental natural frequencies of both design schemes

Twin box girder design scheme	Fundamental lateral bending frequency (Hz)		Fundamental vertical bending frequency (Hz)		Fundamental torsional vibration frequency (Hz)	
	Symmetric	Asymmetric	Symmetric	Asymmetric	Symmetric	Asymmetric
Deep scheme	0.0354	0.0591	0.0691	0.0827	0.1434	0.1498
Shallow scheme	0,0467	0.0797	0.0630	0.0806	0.1536	0.1365

Table 9 Equivalent mass and mass moment of both design schemes

Twin box girder design scheme	Equivalent mass (10^3 kg/m)				Equivalent mass moment (10^3 kg·m^2/m)	
	Fundamental lateral bending		Fundamental vertical bending		Fundamental torsional vibration	
	Symmetric	Asymmetric	Symmetric	Asymmetric	Symmetric	Asymmetric
Deep scheme	105.9	87.20	120.2	115.5	20440	22230
Shallow scheme	109.3	133.0	139.8	155.8	66410	55220

Based on the fundamental symmetric natural frequencies in Table 8 and the corresponding equivalent mass and mass moment in Table 9, the wind tunnel tests were carried out on the 1:80 sectional models of both design schemes. The experimental results of the flutter critical wind speeds with different angles of attack are listed and compared in Table 10. The minimum flutter critical speed is 82m/s for the

deep twin box girder scheme and 93m/s for the shallow twin box girder scheme, respectively. Since the flutter checking speed of Sunda Strait Bridge is set to 93m/s, the aerodynamic flutter stability performance of both design schemes may need to be further improved in the next design stage. It is suggested that the further improvement can be realized by either increasing the width or ventilation ratio of central slot or adopting additional central stabilizer like the combination of stabilizer and slot in Akashi Kaikyo Bridge (Zhou et al., 2015a).

Table 10 Flutter critical speed of both design schemes

Twin box girder design scheme	Flutter critical speed (m/s) Angle of attack			Minimum speed (m/s)	Checking Speed (m/s)
	-3°	0°	+3°		
Deep scheme	84	87	82	82	93
Shallow scheme	93	108	113	93	93

3.3 Widely slotted twin box girder in Taiwan Strait Bridge

As a long-time dream and an engineering challenge, the technology of bridging larger obstacles has entered into a new era of crossing wider sea straits, for example, Messina Strait in Italy, Taiwan Strait in China, Tsugaru Strait in Japan, and Gibraltar Strait linking the European and African Continents. One of the most interesting challenges has been identified as bridge span length limitation, in particular the span limits of suspension bridges as a bridge type with potential longest span. The dominant concerns of super long-span bridges to bridge designers are basically technological feasibility and aerodynamic considerations. With the emphasis on aerodynamic stabilization for longer span length, a typical three-span suspension bridge with a 5,000m central span and two 1,600m side spans is considered as the limitation of span length for Taiwan Strait as shown in Fig. 16.
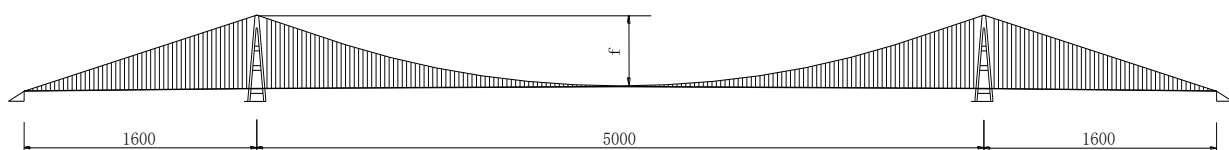

Fig. 16 Elevation of the 5,000m spanned suspension bridge (Unit: m)

In order to push up the aerodynamic stability limit, two kinds of generic deck sections, namely a widely slotted deck (WS) without any stabilizers (Fig. 17a) and a narrowly slotted deck with vertical and horizontal stabilizers (NS) (Fig. 17b), were investigated. The WS cross section has a total deck width of 80m and four main cables for a 5,000m-span suspension bridge while the NS provides a narrower deck solution of 50m and two main cables (Xiang & Ge, 2003; Ge & Xiang, 2006b).

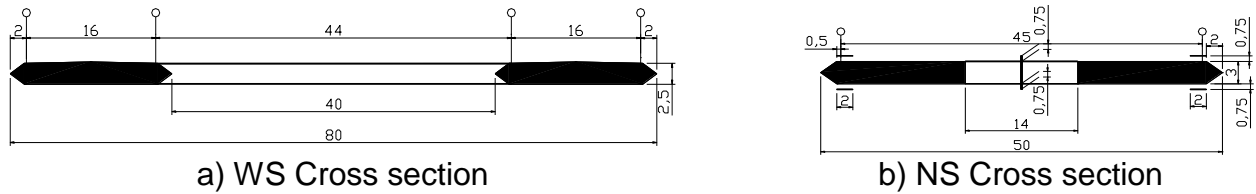a) WS Cross section   b) NS Cross section

Fig. 17 Geometry of deck sections of WS and NS (Unit: m)

Having performed a dynamic finite-element analysis based on the structural parameters listed in Table 11, the fundamental natural frequencies of the structures have been calculated for all four ratios n of cable sag to span and the two deck configurations in Table 12. The fundamental lateral bending frequencies vary about 16% for the WS section and 17% for the NS section from $n = 1/8$ to $n = 1/11$, but almost remain the same between the WS and NS deck configurations. The fundamental vertical bending frequencies are not influenced significantly by both deck configurations and the sag-span ratios. The fundamental torsional frequencies vary differently with the ratio n in the two deck configurations, in which the frequency values go up in the WS section and go down in the NS section with the decrease of the ratio n, but it is interesting to see that the frequency ratio of torsion to vertical bending monotonically decreases with reduction of the ratio n.

Table 11 Parameters of stiffness and mass of the 5,000m suspension bridge

Section	Main Cables			Stiffening Girder			
	EA (Nm^2)	m (kg/m)	I_m (kgm^2/m)	EI_y (Nm^2)	GI_d (Nm^2)	m (kg/m)	I_m(kgm^2/m)
WS	$0.61{\sim}1.12{\times}10^6$	$2.62{\sim}4.82{\times}10^4$	$2.36{\sim}4.33{\times}10^7$	$4.7{\times}10^{11}$	$2.8{\times}10^{11}$	24000	$2.16{\times}10^7$
NS	$0.61{\sim}1.12{\times}10^6$	$2.62{\sim}4.82{\times}10^4$	$1.27{\sim}2.33{\times}10^7$	$8.1{\times}10^{11}$	$4.1{\times}10^{11}$	24000	$5.40{\times}10^6$

Table 12 Fundamental natural frequencies of the 5,000m suspension bridge

Ratio	Lateral (Hz)		Vertical (Hz)		Torsional (Hz)		Frequency Ratio	
	WS	NS	WS	NS	WS	NS	WS	NS
$n = 1/8$	0.02199	0.02156	0.05955	0.05936	0.07090	0.09073	1.191	1.528
$n = 1/9$	0.02322	0.02285	0.06126	0.06115	0.07207	0.08928	1.176	1.460
$n = 1/10$	0.02438	0.02406	0.06219	0.06204	0.07268	0.08653	1.168	1.395
$n = 1/11$	0.02548	0.02520	0.06237	0.06219	0.07269	0.08403	1.165	1.351

With the dynamic characteristics given above and the numerically identified flutter derivatives, the critical wind speeds of the suspension bridges were calculated by multi-mode flutter analysis assuming a structural damping ratio of 0.5%. The results of critical wind speeds together with the generalized mass and mass moment of inertia are summarized in Table 13. For both deck sections the critical wind speed increases with decrease of the ratio n, although the frequency ratio of torsion to vertical bending slightly decreases. The most important reason is the considerable increase of the

generalized properties in the aerodynamic stability analysis. The minimum critical wind speeds for the WS and NS sections are 82.9 m/s and 74.7 m/s, respectively (Ge & Xiang, 2006a; Ge & Xiang, 2007).

Table 13 Critical flutter wind speeds of the 5,000m suspension bridge

Ratio	m ($\times 10^4$kg/m)		I_m ($\times 10^7$kgm^2/m)		f_h (Hz)		f_α (Hz)		U_{cr} (m/s)	
	WS	NS	WS	NS	WS	NS	WS	NS	WS	NS
$n = 1/8$	6.01	6.79	5.28	2.37	0.05955	0.05936	0.07090	0.09073	82.9	74.7
$n = 1/9$	6.27	7.43	5.36	3.22	0.06126	0.06115	0.07207	0.08928	88.8	77.4
$n = 1/10$	6.73	8.33	5.92	3.29	0.06219	0.06204	0.07268	0.08653	90.9	78.9
$n = 1/11$	7.66	9.52	6.77	3.62	0.06237	0.06219	0.07269	0.08403	98.9	82.7

4. AERODYNAMIC CONCERNS OF LONG-SPAN CABLE-STAYED BRIDGES

Ten longest-span cable-stayed bridges completed in the world are given in Table 14, including six in China and one in Russia, Japan, France and Korea, respectively (Internet address B 2016). All ten cable-stayed bridges have suffered in cable RWIV, but no other aerodynamic problem. In order to improve cable RWIV, either dimples or spiral wires on cable surfaces, sometimes together with dampers, have been used to reduce water rivulet. Aerodynamic concerns of long-span cable-stayed bridges are not only related to dynamic and aerodynamic characteristics of the bridges, but also RWIV of stay cables, which are discussed in the following sections.

Table 14 Ten longest-span cable-stayed bridges completed in the world

Span Order	Bridge Name	Main Span	Girder Type	Wind-Induced Problem	Control Measure	Country	Year Built
1	Russky	1104m	Box	Cable RWIV	Spiral wires	Russia	2012
2	Sutong	1088m	Box	Cable RWIV	Dimples	China	2008
3	Stonecutters	1018m	Twin-box	Cable RWIV	Dimples	China	2009
4	Edong	926m	P.K. Box	Cable RWIV	Spiral wires	China	2010
5	Tatara	890m	Box	Cable RWIV	Dimples	Japan	1999
6	Normandy	856m	Box	Cable RWIV	Spiral wires	France	1995
7	2nd Jiujiang	818m	Twin-box	Cable RWIV	Spiral wires	China	2013
8	Jingyue	816m	P.K. Box	Cable RWIV	Spiral wires	China	2010
9	Inchoen	800m	Box	Cable RWIV	Dimples	Korea	2009
10	Xiazhang	780m	Box	Cable RWIV	Spiral wires	China	2013

4.1 Dynamic characteristics of long-span cable-stayed bridges

Cable-stayed bridge has become the most popular type of long-span bridges in China for the past two decades. In 1993, Shanghai Yangpu Bridge with the main span of 602 m once became the longest span cable-stayed bridge in the world. Although this record was quickly surpassed by Normandy Bridge in 1995 and Tatara Bridge in 1999, China already has built three record-breaking span length cable-stayed bridges, including the 1088m Sutong Bridge in 2008, the 1018m Hong Kong Stonecutters Bridge in 2009 and the 926m Hubei Edong Bridge in 2010 (Ge & Xiang, 2007).

Sutong Bridge, connecting Suzhou City and Nantong City over Yangtze River in Eastern China, consists of seven steel deck spans including a 1088 m long central span and three spans on both sides. The cross-section of the deck is a streamlined orthotropic steel box, 35.4 m wide and 4 m deep, with two vertical webs required by the longitudinal load distribution. This box-girder carries three 3.75 m wide lanes of traffic in each direction with 3.5 m wide hard shoulders to provide an emergency parking zone shown in Fig. 18. Stonecutters Bridge is composed of nine spans including a 1018m long central span with steel deck and four spans on both sides with concrete deck. The cross-section of steel deck is twin streamlined orthotropic steel boxes, 2x15.9m wide and 3.9m deep. This twin box girder carries three traffic lanes of 11m width in each direction with 3.3m wide hard shoulders for emergency parking shown in Fig. 19. Edong Bridge over Yangtze River is also a nine span hybrid cable-stayed bridge with a 926m long central span with steel deck. After having made the comparison of dynamic and aerodynamic characteristics with a traditional closed box, the cross-section of steel deck is designed as two separate box girder with the total deck width of 34.4m and the depth of 3.8m, without the bottom plate of a box at the central part to save steel material, shown in Fig. 20.
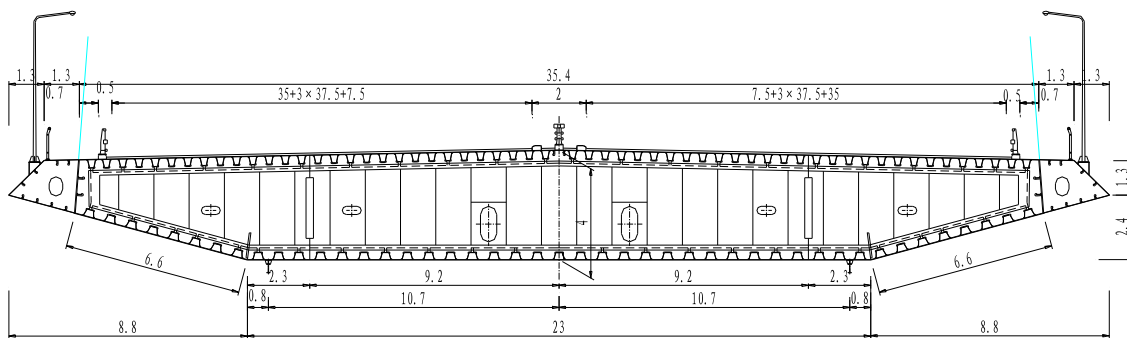

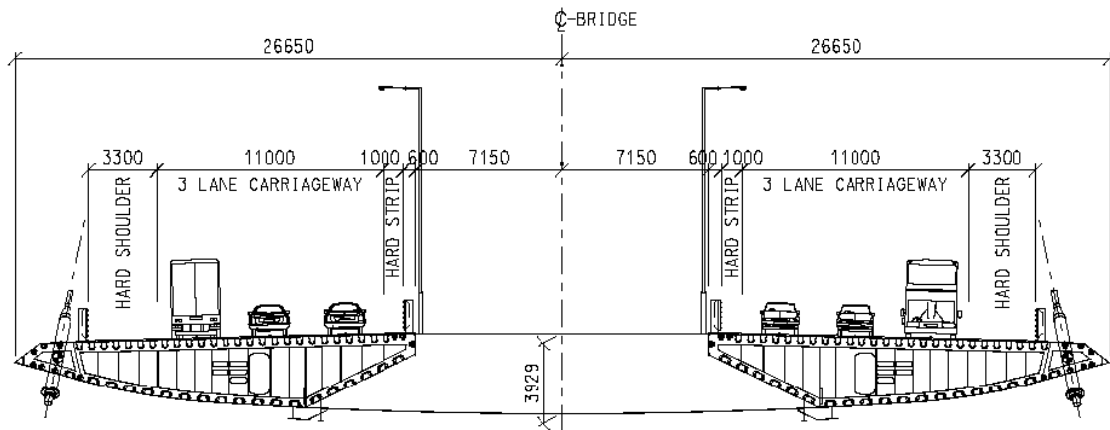Fig. 18 Deck cross-section of Sutong Bridge (Unit: m)

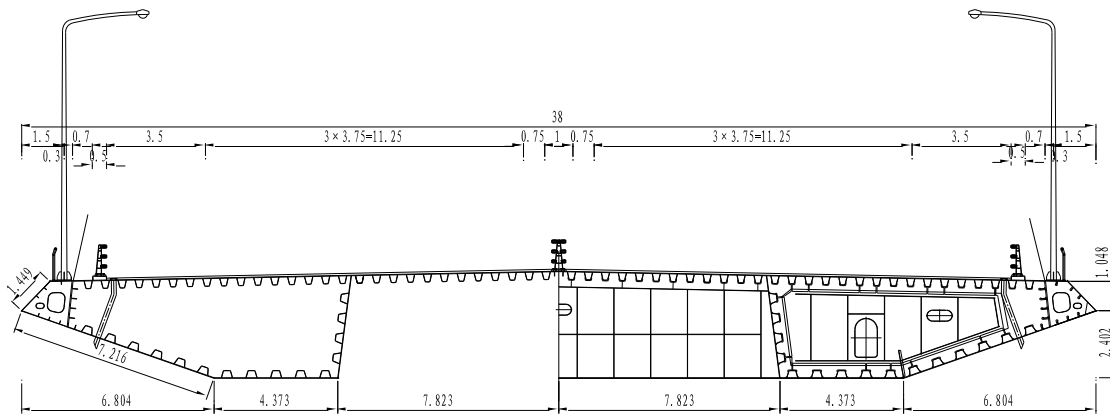Fig. 19 Deck cross-section of Stonecutters Bridge (Unit: mm)

Fig. 20 Deck cross-section of Edong Bridge (Unit: m)

In order to study dynamic characteristics of these long-span cable-stayed bridges, finite-element-method is usually adopted to solve natural frequencies of an idealized structure. The finite-element idealization of a cable-stayed bridge is basically attempted with finite beam elements for longitudinal girder, transverse beams and pylon elements, and cable elements considering geometric stiffness for stay cables, and geometric dimensions and material properties for these elements should be correctly provided. Having performed a dynamic finite-element analysis, the first several natural frequencies of a cable-stayed bridge can be extracted, and the most important figures are those related to the fundamental vibration frequencies, including lateral bending, vertical bending and torsion modes. The fundamental frequencies of lateral bending, vertical bending and torsion modes of five cable-stayed bridges with a main span over 800m are collected and compared in Table 15. Among these five bridges, Tatara Bridge is an exceptional case always with the smallest values of the fundamental frequencies because of the least depth and width of the box girder, but with the largest ratio of the torsional frequency to the vertical frequency. With the unique twin box girder, Stonecutters Bridge has the next smallest fundamental frequencies of lateral and

vertical bending modes, but almost the same torsional frequency as Tatara Bridge and Normandy Bridge. As the longest cable-stayed bridge, Sutong Bridge even has the higher torsional frequency than the other four bridges. It should be concluded that there is not any clear tendency that fundamental frequencies decrease with the increase of span length of cable-stayed bridges (Ge and Xiang, 2008).

Table 15 Fundamental frequencies of five long-span cable-stayed bridges

Span Order	Bridge Name	Main Span (m)	Lateral Freq. (Hz)	Vertical Freq. (Hz)	Torsional Freq. (Hz)
1	Sutong	1088	0.104	0.196	0.565
2	Stonecutters	1018	0.090	0.184	0.505
3	Edong	926	0.153	0.235	0.548
4	Tatara	890	0.078	0.139	0.497
5	Normandy	856	0.151	0.222	0.500

4.2 Aerodynamic stability of long-span cable-stayed bridges

The most important aerodynamic characteristic is flutter instability, which can be evaluated by simply comparing critical flutter speed with required wind speed. Critical flutter speed of a bridge can be determined through direct experimental method with sectional model or full aeroelastic model and computational method with experimentally identified flutter derivatives, and required wind speed is based on basic design wind speed multiplied by some modification factors, for example, considering deck height, gust speed, longitudinal correlation of wind speed, safety factor of flutter, and so on. Both the critical flutter speeds and the required wind speeds of these five bridges are shown in Table 16. It is very surprised to see that both critical flutter speeds and required wind speeds steadily increase with the increase of main span. Although the reason for this kind of tendency is still under investigation, the fact that critical flutter speed is not so sensitive to main span may support to make another jump in span length of cable-stayed bridges in the near future (Ge and Xiang, 2008).

Table 16 Aerodynamic stability of five long-span cable-stayed bridges

Span Order	Bridge Name	Main Span (m)	Frequency Ratio (Tors./Vert.)	Flutter Speed (m/s)	Required Speed (m/s)
1	Sutong	1088	2.88	88.4	71.6
2	Stonecutters	1018	2.74	140	79.0
3	Edong	926	2.33	81.0	58.6
4	Tatara	890	3.58	80.0	61.0
5	Normandy	856	2.25	78.0	58.3

4.3 Wind and rain induced vibration of stay cables

One of the most challenging problems suffered in these long-span cable-stayed bridges listed in Table 14 is long stay cable aerodynamics under windy and/or rainy

weather conditions. The wind tunnel testing of prototype cable sections was carried out in dry-wind and rain-wind situations, for example, Sutong Bridge, in particular for the outer diameters of 139mm (the most popular cables) and 158mm (the longest cables). As a basic result, cable vibration is much severe under the rain-wind condition than under the dry-wind condition for both cable sections shown in Fig. 21, and the maximum amplitudes of these two cables exceed the allowable value of length/1700 (Ge, et al., 2004). It should be mentioned, however, that the amplitude of rain-wind cable vibration lies on several main factors, and one of the most important factors is spatial cable state, usually described by inclined angle of a cable, α, and yawed angle of wind flow, β. Fig. 22 gives the comparison results, from which the most unfavorable spatial state of a ϕ139 cable is under the inclined angle of $\alpha = 35°$ and the yawed angle of $\beta = 20°$, and the wind speed is about 6m/s to 9m/s (Ge, 2011).
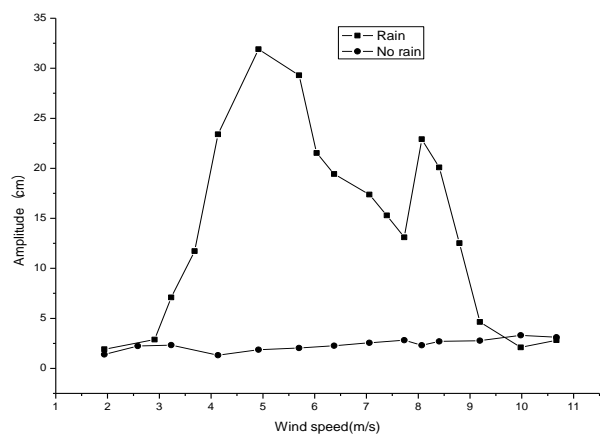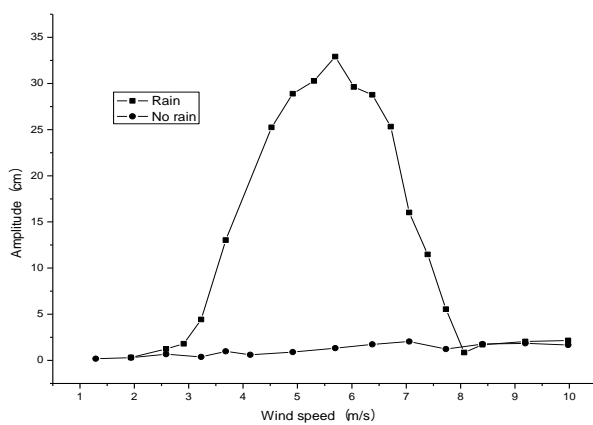
a) Φ139 stay cable b) Φ158 stay cable
Fig. 21 Cable vibration under dry-wind and rain-wind conditions
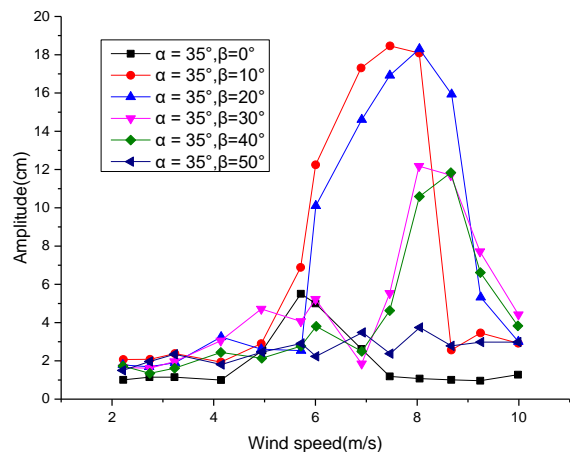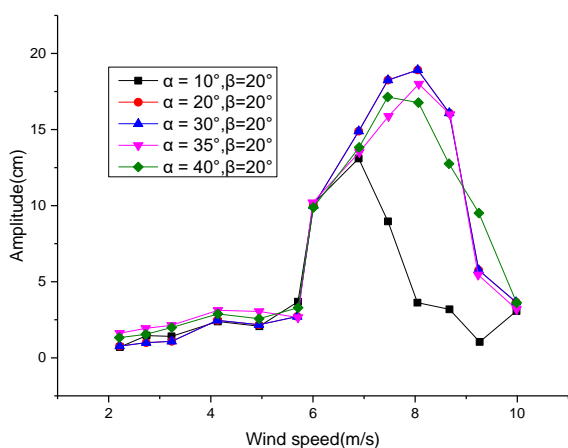
a) Inclined angle influence b) Yawed angle influence
Fig. 22 Wind-rain induced cable vibration under different spatial states

In order to reduce sever rain-wind induced cable vibration, cable damping has been investigated together with cable vibration frequency. Based on various on-site measurement of cable damping, the average value of cable damping ratio is about

0.15%. Four kinds of damping ratios and four types of vibration frequencies have been tested, and the main results are presented in Fig. 23. It can be expected that rain-wind induced cable vibration can be effectively controlled with doubled average damping ratio up to 0.30%, for which numerous damping devices have been produced based on different mechanism, for example, oil pressure, oil viscous shearing, friction, rubber viscosity, magnetic resistance, electrical resistance, and so on (Ge, 2011).

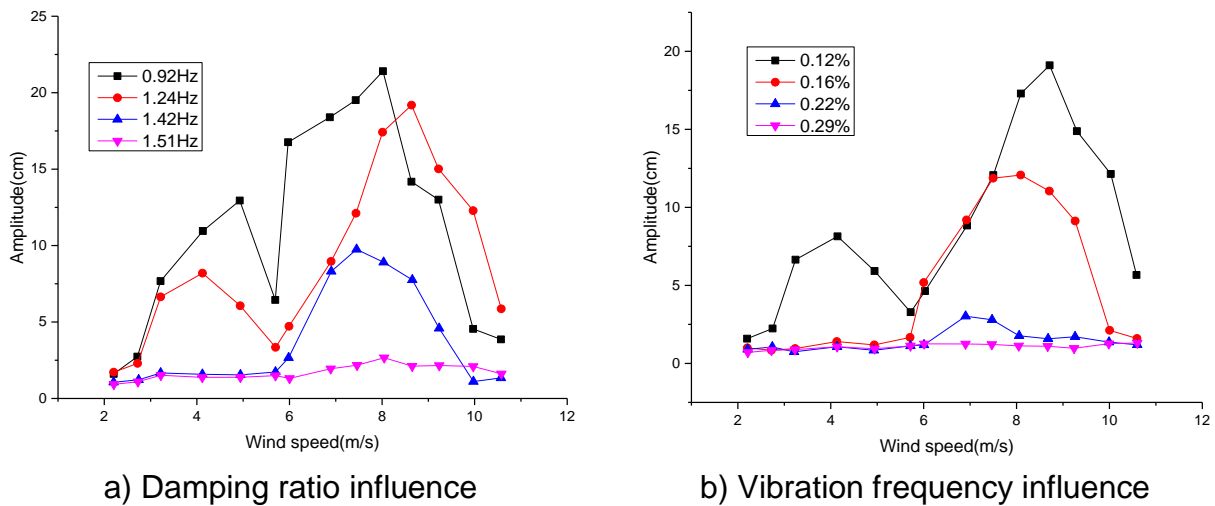a) Damping ratio influence   b) Vibration frequency influence
Fig. 23 Wind-rain induced cable vibration with different damping ratios and frequencies

Another way to ease rain-wind vibration is to prevent cable surface from forming rivulets, which are known as a main effect to generate cable vibration. Two kinds of aerodynamic countermeasures including spiral wires and dimples against rivulets on cable surface were tested and were proven to be sufficient to mitigate vibration amplitude less than the requirement shown in Fig. 24. The cable cross ties are also effective to reduce cable vibration not only rain-wind induced but also other vibration, but have been adopted in a very few cable-stayed bridges, for example, Normandy Bridge, one out of ten longest cable-stayed bridges, because of complicated connection with stay cables (Ge, 2011).
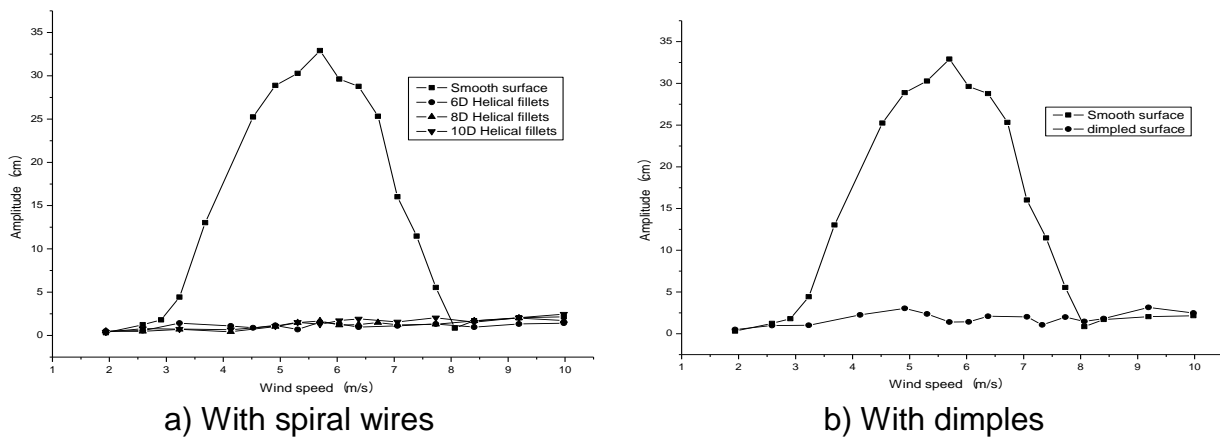

a) With spiral wires   b) With dimples
Fig. 24 Aerodynamic countermeasures of wind-rain induced cable vibration

5. FEASIBLE STABILIZING LONGER CABLE-STAYED BRIDGES

As mentioned in the previous section, the span limitation of cable stayed bridges for aerodynamic flutter concerns seems to be not reached yet. In order to explore the aerodynamic limit span length, two super long cable-stayed bridges, one with single 1,400m span and the other with double 1,500m spans, have been experimentally investigated through sectional and full aeroelastic models in flutter and torsional instability.

5.1 Single 1,400m span cable-stayed bridge

The span arrangement of the proposed design scheme for a single 1,400m span cable-stayed bridge is set to be 180+156+300+1400+300+156+180 m as shown in Fig. 25. The two concrete towers are 357m high, and the steel box deck is originally 41m wide and 4.5m deep, also shown in Fig. 25. The fundamental natural frequencies of the lateral bending, the vertical bending and the torsional vibration of bridge deck obtained via a FEM modal analysis are 0.0611Hz, 0.1474Hz and 0.4157Hz, respectively, for the completion bridge state. The corresponding modal equivalent masses and mass moment of the bridge deck are 29,087 kg/m, 32,894 kg/m and 4,606,300 kgm^2/m, respectively (Zhu et al., 2011).
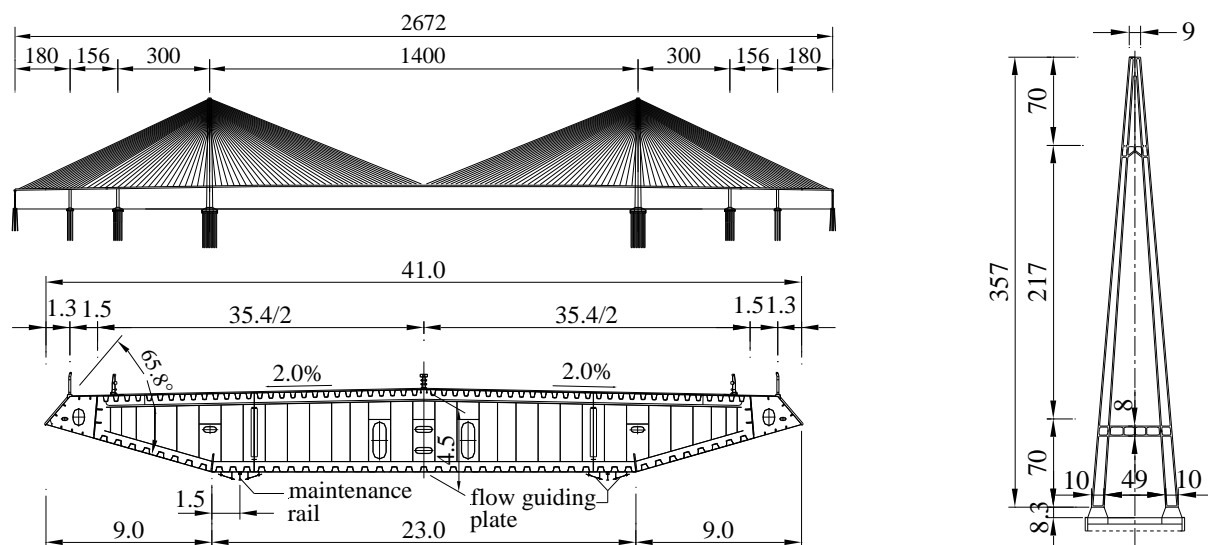

Fig. 25 General arrangement of a single 1,400m span cable-stayed bridge (unit: m)

The flutter performance of the original deck scheme was firstly investigated with a 1:70 scaled down sectional model wind tunnel test under smooth flows for three wind attack angles of +3°, 0°and -3°. The corresponding tested flutter critical wind speeds are 58m/s, 104m/s and >110m/s, respectively. This indicates that the +3° wind attack angle is the most unfavorable condition for aerodynamic flutter instability of the proposed bridge design scheme, and the lowest critical wind speed of 58m/s is much smaller than the desired flutter checking speed of 80m/s (Zhu et al., 2011).

In order to improve the aerodynamic flutter performance, the further wind tunnel tests were conducted on four kinds of aerodynamic counter measures, including the

upper central stabilization plate (UCSP) with the height of 1.5m, the combination of the upper and lower central stabilization plate (ULCSP) with the both heights of 1.5m, the cantilever horizontal stabilization plate (CHSP) at the nose tips of both wind fairings with the widths of 1.0m, 1.2m, 1.5m, 1.7m and 2.0m, and the central slotting (CS) with the gap widths of 0.1B, 0.15B and 0.2B, shown in Fig. 26. The general testing results indicate that both the UCSP and ULCSP measures play little influence on the flutter performance, and the measures of CS exerts negative effect on the flutter performance of the bridge when the gap width is below 0.15B, and can raise the flutter critical wind speed up to 74m/s (28%) when the gap width increases to 0.2B, but it is still below 80m/s. The most effective counter measure is the CHSP with the optimal width of 1.5m, by which the flutter critical speed can be significantly raised from 58m/s to 110m for +3°, slightly decreases from 104m/s to 96m/s for 0°, and keeps greater than 110m/s for -3°, in which the 0° wind attack angle becomes the most unfavorable condition for aerodynamic flutter instability (Zhu et al., 2011).

Original design + UCSP (h=1.5m)   Original design + CHSP(1.0,1.2,1.5,1.7,2.0m)

Original design + ULCSP (h=1.5m)   Central Slotting (0.1B, 0.15B, 0.2B)
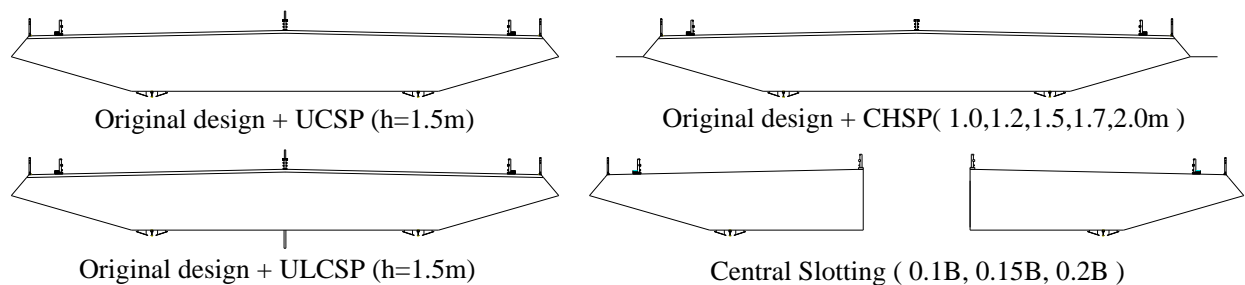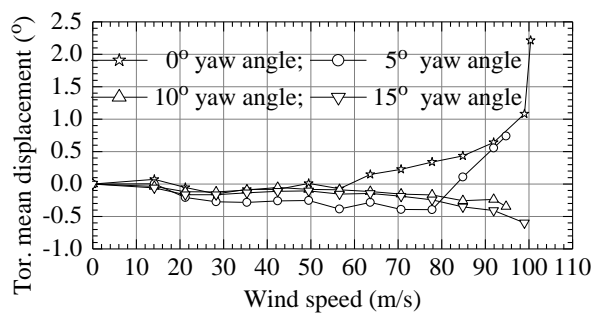
Fig. 26 Four kinds of aerodynamic counter measures

To investigate the three-dimensional effect of bridge deformation and vibration on the flutter performance, the confirmation wind tunnel test with a full bridge aeroelastic model with the scale of 1:200 was finally carried out under smooth flows at the wind attack angles of +3°, 0°and -3° and the yaw angle of 0°, 5°, 10° and 15°. Both aerodynamic flutter instability and aerostatic torsional divergence occurred under different combinations of attack angle and yaw angle. The minimum flutter critical speed was found under the attack angle of -3° and the yaw angle of 0°, and the lowest torsional critical speed was recorded under the attack angle of 0° and the yaw angle of 0°, shown in Fig. 27 (Zhu et al., 2011).
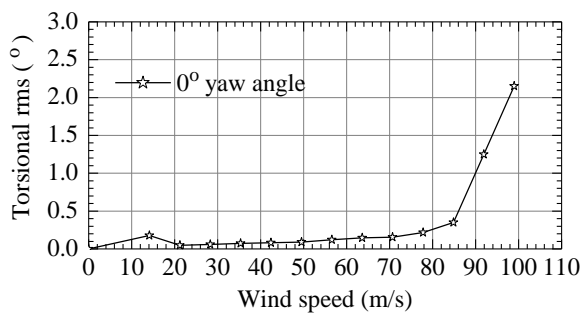
a) RMS displacement at -3° attack angle   b) Mean displacement at 0° attack angle
Fig. 27 Torsional displacements at the mid span of full aeroelastic model

It should be noted that the flutter critical speeds obtained via full bridge aeroelastic model testing are evidently lower than those gained via sectional model testing by 10~20%, and the vibration mode approaching flutter of the bridge deck showed a strong coupling behavior not only in the torsional and vertical degrees, but also in the lateral degree. These phenomena have rarely been reported in the past wind-resistance study of the cable-stayed bridges with a main span short than 1,100m. The above-mentioned interaction between wind-induced static and dynamic instabilities may be one of the reasons for the difference of flutter critical speeds. The large lateral deformation of the bridge structures due to static action of wind and the significant lateral vibration of the very long cables, which were observed in the full bridge aeroelastic model test of the 1,400m spanned bridge but not in other shorter bridges, must be the other reason. However, the mechanisms of how the above-mentioned factors advance the onset points of the static and dynamic instabilities is not clear yet and needs to investigate (Zhu et al., 2011).

5.2 Double 1,500m spans cable-stayed bridge

The double 1,500m spans cable-stayed bridge has been proposed for the main navigational channel of Qiongzhou Strait Bridge, which connects Zhanjiang City, Guangdong Province in the mainland of China, and Haikou City, Hainan Province in the largest island of China, called Hainan Island. The span arrangement is designed as 244+408+1500+1500+408+244 m, and the twin box deck is adopted with the total width of 60.5m including a 14m central slot, shown in Fig. 28. The fundamental natural frequencies of the lateral bending, the vertical bending and the torsional vibration of bridge deck obtained via a FEM modal analysis are 0.0810Hz, 0.1235Hz and 0.3524Hz, respectively, for the completion bridge state. The corresponding modal equivalent masses and mass moment of the bridge deck are 39,020 kg/m, 54,370 kg/m and 15,699,500 kgm^2/m, respectively (Zhou et al., 2015b).

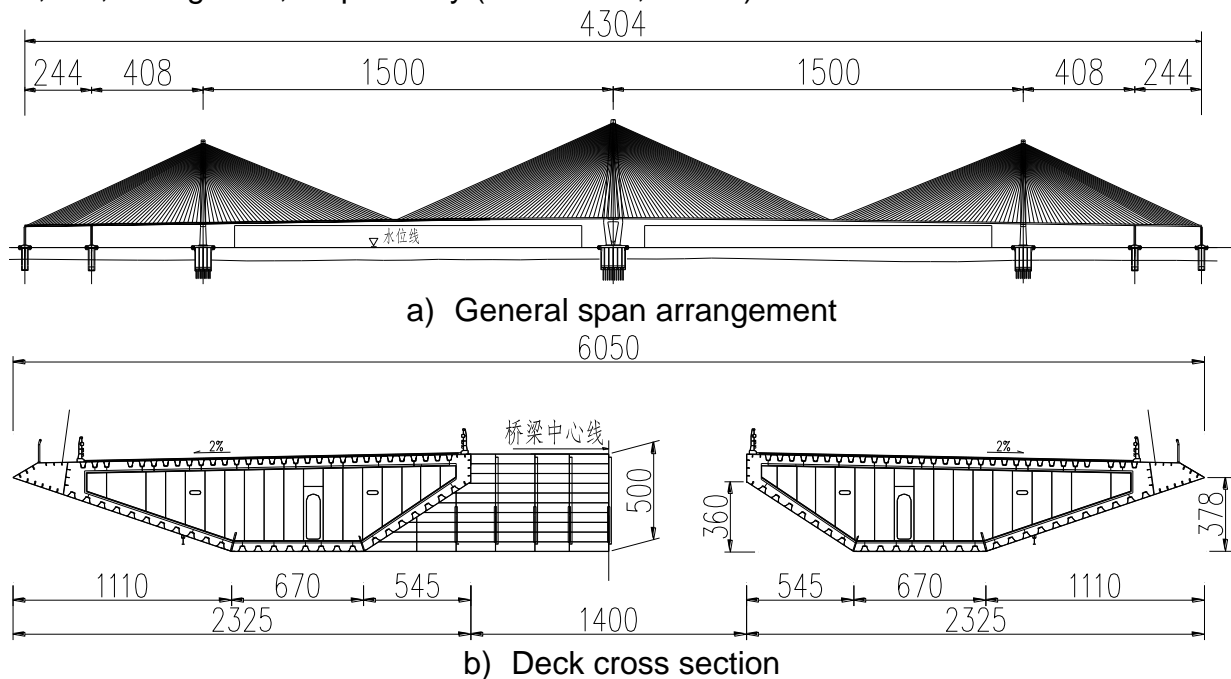a) General span arrangement

b) Deck cross section
Fig. 28 General arrangement of a double 1,500m spans cable-stayed bridge (unit: m)

The flutter performance of the bridge was firstly studied through wind tunnel testing with a 1:80 sectional model under smooth flows at three wind attack angles of +3°, 0°and -3°. The corresponding tested flutter critical wind speeds are all over 118m/s, which is much larger than the desired flutter checking speed of 93m/s for this typhoon prone area (Zhou et al., 2015b).

In order to investigate the three-dimensional effect of bridge deformation and vibration on aerodynamic flutter instability and aerostatic torsional divergence, which was raised by the previous 1,400m spanned cable-stayed bridge, the further wind tunnel testing with a 1:320 full bridge aeroelastic model was carefully conducted under smooth flows at the wind attack angles of +3°, 0°and -3°. The mean values and standard deviation values (STD) of the torsional displacement at mid span are plotted in Fig. 29. The corresponding critical wind speeds for aerodynamic flutter instability and aerostatic torsional divergence are listed in Table 17. It can be seen from Table 17 that the critical wind speeds due to aerostatic torsional divergence are already smaller than those due to aerodynamic flutter instability, which means that the structural resistance to wind-induced aerodynamic and aerostatic instabilities of such a long cable-stayed bridge with a twin box deck becomes very close to each other. This phenomenon together with the interaction between these two kinds of instabilities should be seriously taken into account in the future design (Zhou et al., 2015b).
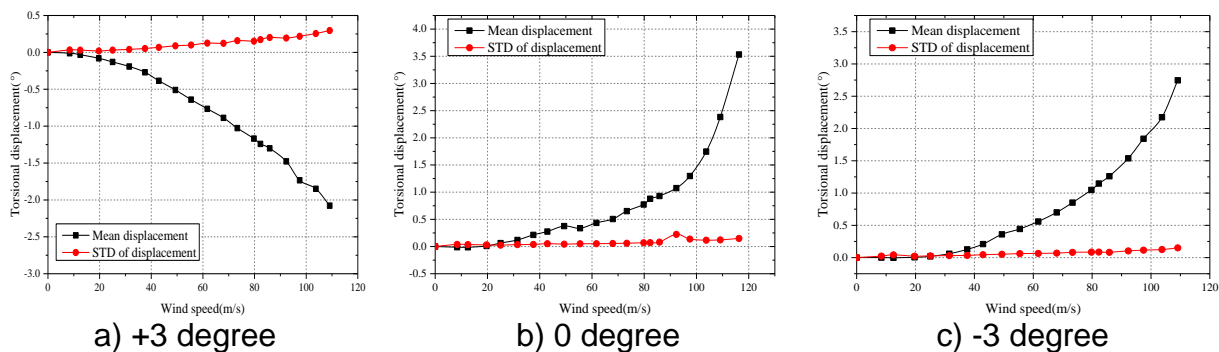

a) +3 degree   b) 0 degree   c) -3 degree

Fig. 29 Torsional displacements at mid span

Table 17 Critical wind speeds for flutter instability and torsional divergence

Angle of attack (°)	Aerodynamic flutter instability		Aerostatic torsional divergance	
	Critical speed (m/s)	Checking speed (m/s)	Critical speed (m/s)	Checking speed (m/s)
+3	>202		109	
0	>210	93	116	91
-3	>118		>109	

6. CONCLUSIONS

With the experience gained from the recently built long-span suspension bridges, such as Runyang Bridge with central stabilizer, Xihoumen Bridge with twin box deck and Akashi Kaykyo with the combination of stabilizer and slot, the intrinsic limit of span length due to aerodynamic stability is about 1,500m for a traditional suspension bridge with either a streamlined box deck or a ventilated truss girder. Beyond or even approaching this limit, designers should be prepared to improve aerodynamic performance by adopting some countermeasures, including shaping box girder, vertical and/or horizontal stabilizer and twin box girder. Based on a preliminary study, either a widely slotted twin box girder or a narrowly slotted girder with vertical and horizontal stabilizers could provide a 5,000m span-length suspension bridge with high enough critical wind speed, which can meet aerodynamic requirement in most typhoon-prone areas in the world.

The engineering practice of the latest record-breaking cable-stayed bridges, including Sutong Bridge, Stonecutters Bridge and Edong Bridge, unveils the facts that traditional long-span cable-stayed bridges with spatial cable plane and steel box girder have high enough critical flutter speed and the main aerodynamic concern is rain-wind induced vibration of long stay cables. Through the investigation of a single 1,400m span cable-stayed bridge and a double 1,500m spans cable-stayed bridge, however, the traditional cable-stayed bridges may come to their span length limitation of 1,400m or 1,500m due to wind resistance, and both aerodynamic flutter instability and aerostatic torsional divergence must be carefully considered for both single and twin box girder in the future design.

REFERENCES

Chen, A.R., Guo, Z.S., Zhou, Z.Y., Ma, R.J and Wang, D.L. (2002), Study of Aerodynamic Performance of Runyang Bridge, *Technical Report WT200218, State Key Laboratory of Disaster Reduction in Civil Engineering at Tongji University (in Chinese).*

Ge, Y.J., Yang, Y.X., Cao, F.C. and Zhao, L. (2003), Study of Aerodynamic Performance and Vibration Control of Xihoumen Bridge, *Technical Report WT200320, State Key Laboratory of Disaster Reduction in Civil Engineering at Tongji University (in Chinese).*

Ge, Y.J. and Xiang, H.F. (2006a), "Outstanding Chinese steel bridges under construction," *Proceedings of the 6th International Symposium on Steel Bridges, Prague, Czech Republic, June 1-3,* 2006.

Ge, Y.J. and Xiang, H.F. (2006b), "Tomorrow's challenge in bridge span length," *Proceedings of the IABSE Symposium 2006, Budapest, Hungary, September 13-15,* 2006.

Ge, Y.J. and Xiang, H.F. (2007), "Great demand and various challenges - Chinese Major Bridges for Improving Traffic Infrastructure Nationwide," *Keynote paper in Proceedings of the IABSE Symposium 2007, Weimar, Germany, September 19-21,* 2007.

Ge, Y.J. and Xiang, H.F. (2008), "Aerodynamic challenges in long-span bridges," *Proceedings of the Centenary Conference of the Institution of Structural Engineers*, *Hong Kong, China, January 24-26, 2008.*

Ge, Y.J. (2011), "Wind and rain induced effects on typical prisms and stay cables," *Keynote paper in Proceedings of the 5th International Symposium on Wind Effects on Buildings and Urban Environment*, *Tokyo, Japan, March 7-8*, 2011.

Ge, Y.J., Yang, Y.X., Cao, F.C. and Zhao, L. (2015), Preliminary Study of Aerodynamic Performance and Vibration Control of Shuangyumen Bridge, *Technical Report WT201503, State Key Laboratory of Disaster Reduction in Civil Engineering at Tongji University (in Chinese).*

Internet address A (2016), http://en.wikipedia.org.wiki//List_of_longest_suspension_bridges

Internet address B (2016), http://en.wikipedia.org.wiki//List_of_the_largest_cable-stayed_bridges

Makoto, K. (2004), "Technology of the Akashi Kaikyo Bridge", *Structural Control and Health Monitoring*, **11**, 75-90.

Miyata, T. (2003), "Historical review of long-span bridge aerodynamics", *Journal of Wind Engineering and Industrial Aerodynamics*, **91**, 1393-1410.

Xiang, H.F. and Ge, Y.J. (2003), "On aerodynamic limit to suspension bridges," *Proceedings of the 11th International Conference on Wind Engineering, Texas, USA, June 2-5, 2003.*

Zhou, Z.Y., Song, J.Z., Hu, X.H. and Ge, Y.J. (2015a), Sectional Model Testing of Stiffening Girder of Sunda Strait Bridge, *Technical Report WT201506, State Key Laboratory of Disaster Reduction in Civil Engineering at Tongji University (in Chinese).*

Zhou, Z.Y., Hu, X.H. and Ge, Y.J. (2015b), Wind Tunnel Study on Wind Resistance of Qiongzhou Strait Bridge, *Technical Report WT201510, State Key Laboratory of Disaster Reduction in Civil Engineering at Tongji University (in Chinese).*

Zhu, L.D., Zhang, H.J., Guo, Z.S. and Hu, X.H. (2011), "Flutter performance and control measures of a 1400m-span cable-stayed bridge scheme with steel box deck," *Proceedings of the 13th International Conference on Wind Engineering*, Amsterdam, *The Netherlands, July 10-15*, 2011.